

# RADIO ASTRONOMICAL IMAGE FORMATION USING SPARSE RECONSTRUCTION TECHNIQUES

Runny Levanda<sup>1</sup> \*

Amir Leshem<sup>1,2</sup>

<sup>1</sup>School of Engineering  
Bar-Ilan University,  
Ramat-Gan, 52900, Israel

<sup>2</sup>Faculty of EEMCS  
Delft University of Technology,  
Delft, The Netherlands

## ABSTRACT

In this paper we present a sparse reconstruction algorithm for the deconvolution of Radio astronomical synthesis images. We present the deconvolution problem as an  $\ell_1$  optimization. Using the sparsity of the astronomical image we obtain that the  $\ell_1$  reconstruction recovers the sparse image consistent with the observed data. We end up with a simulated example of the reconstruction, using a simulated radio telescope array.

**Index Terms**— Radio astronomy, images reconstruction, deconvolution algorithm,  $\ell_1$

## 1. INTRODUCTION

High sensitivity, fine resolution, and robust immunity to terrestrial interference, are the requirements from modern radio observations. This never ending quest for improving all those parameters has led to the development of both new instruments and novel signal processing methods. The building of the Square Kilometer Array (SKA) [1] and the Low Frequency Array (LOFAR) [2] are two examples of these advanced instruments. In these two instruments, the pre-processing of the received signal is done in hardware due to the vast amount of data collected by the antennas. Image formation algorithms are implemented in software and are applied to the pre-processed data.

Below, we briefly describe the several radio astronomical imaging techniques. For a more extensive overview the reader is referred to [3].

Two principles dominate the astronomical imaging deconvolution. The first is the CLEAN method proposed by Hogbom [4]. It is an iterative sequential Least-Squares (LS) fitting procedure, in which the brightest source location and power are estimated, to enable its removal from the image. The process then continues to find the next brightest source, and it is also removed. These iterations continue until the residual image is noise-like. and no distinctive source can be observed.

A second approach proposed by Jaynes [5] is the maximum entropy method (MEM). An entropy function is defined so the entropy function maximum is achieved by a positive image with a compressed pixels intensities. There are many different ways to define the entropy [6]. The reconstructed image is the image that fits the measured visibility data and maximizes the defined entropy function. The compressed pixels values leads to smooth images. This idea has also been proposed by Frieden [7] and applied to radio astronomical imaging by Gull and Skilling [8].

Briggs [9] proposed a non-negative least squares approach (NNLS) which eliminates the need for iterative processing. However, the computational complexity is very large. A parametric approach was proposed and discussed by Leshem [10], [11] and by Ben-David [12].

Marsh and Richardson [13] proved that the CLEAN algorithm can be regarded as an approximation to  $\ell_1$  minimization for images with point sources.  $\ell_1$  is not the only criterion. Recovery of noisy and blurred images using total variation (TV) optimization (3) for smooth images is discussed by Dobson and Santosa [14]. Chen et al. [15] deal with  $\ell_1$  minimization of image basis to achieve image sparseness using linear programming. Feuer and Nemirovski [16] and Elad and Bruckstein [17] establish sufficient and necessary condition for replacing  $\ell_0$  optimization (with high computational complexity) by linear programming when searching for the unique sparse representation. Rudelson and Vershynin [18] prove the guarantees for exact reconstruction of a sparse signal from its Fourier measurements. In this paper, we demonstrate how sparse image reconstruction via  $\ell_1$  minimization can be used for the radio astronomical image formation problem. We reduced the  $\ell_1$  optimization problem into linear programming to reduce computational complexity.

## 2. DATA MODEL

Radio Telescopes (RTs) observation method is based on correlations between the signals received at antenna pairs. Fig (1) shows a source observed by such antenna pair, the observation coordinate system i.e.  $(u, v, w)$  and  $(l, m, n)$ . The visibilities

\*Email:ronny\_general@yahoo.com

measured by the radio telescope corresponds to the specific antenna location (the base line length and orientation at the time of the measurement) and the source intensity  $I(l, m)$  can be written as:

$$V(u, v) = \sum_{l=1}^N \sum_{m=1}^N I(l, m) \exp \left[ -\frac{2\pi i}{N}(ul + vm) \right]. \quad (1)$$

where  $N$  is the image size. The measurements location (i.e.  $u, v$  points) determined by the observed source direction, the radio telescope structure and earth rotation. The dirty image can be calculated using the inverse fourier transform, where points in the  $(u, v)$  domain that were not measured by the radio telescope are interpolated using tapering and gridding [6]. The dirty image is given by:

$$I_D(l, m) = \frac{1}{N^2} \sum_{u=1}^N \sum_{v=1}^N V(u, v) \exp \left[ \frac{2\pi i}{N}(ul + vm) \right]. \quad (2)$$

The image  $I(l, m)$  should then be reconstructed from the dirty image  $I_D(l, m)$ .

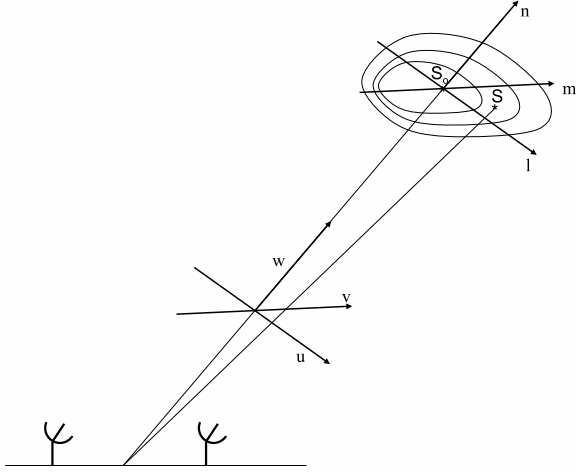


**Fig. 1.** A distance source is observed by antenna pair. The base line connecting the two antennas is the origin of the  $(u, v, w)$  coordinate system. The  $w$  axis is pointing from the base line toward the source reference point.  $(u, v)$  are perpendicular to  $w$  and selected according to earth orientation.  $(l, m, n)$  is a unit vector in the  $(u, v, w)$  system pointing to a specific location in the source (at the source reference point  $l = 0, m = 0$ ), while  $n = \sqrt{(l^2 + m^2)}$ .

### 3. SPARSE RECONSTRUCTION TECHNIQUE

From the nature of a distance source in the sky, many radio telescope images are sparse (i.e. most of the image is empty

/ blank). Candes et al. [19] deal with sparse signal reconstruction from partial knowledge of its fourier transform coefficients when both the signal and the known coefficients are randomly uniformly selected.

Reconstruction of the sparse signal  $g$  is done using one of three cost functions

$$\begin{aligned} P_0 & \min \|g\|_{\ell_0}, \\ P_1 & \min \|g\|_{\ell_1}, \\ TV & \min \|g\|_{TV}, \end{aligned} \quad (3)$$

where  $\|g\|_{\ell_0}$  is the number of non-zero components of  $g$ ,  $\|g\|_{\ell_1}$  is  $\sum_i |g_i|$  and  $\|g\|_{TV}$  is the norm of the derivative of  $g$  in the time domain. And proved the following theorem:

**Theorem 3.1.** Let  $g \in \mathcal{C}^N$  be a discrete signal supported on an unknown set  $T$ , and choose  $\Omega$  uniformly at random. For a given accuracy parameter  $M_{acc}$ , if

$$|T| < C_{M_{acc}} (\log N)^{-1} |\Omega|. \quad (4)$$

Then with probability at least  $1 - O(N^{-M_{acc}})$ , the minimizer to the problem  $P_1$  (3) is unique and equal to  $g$ .

Radio astronomical image reconstruction is done based on the visibility measurement in the  $(u, v)$  domain. Reconstruction of the source image  $\mathbf{I}(l, m)$  is equivalent to estimating the missing visibility points. The missing  $\mathbf{V}(u, v)$  measurements together with the image itself are estimated by minimizing a cost function  $\|\mathbf{I}(l, m)\|_{\ell_1}$  in the  $(l, m)$  domain using the constraints of image positivity and the measured visibility data.

$$\|\mathbf{I}(l, m)\|_{\ell_1} = \sum_{l=1}^N \sum_{m=1}^N I(l, m) \quad (5)$$

since  $I(l, m)$  is a positive quantity. To solve the reconstruction problem fast, we represent the problem as a linear programming problem with real variables. To that end let  $\langle \cdot, \cdot \rangle$  be a one-to-one pairing function mapping  $\{0, \dots, N-1\} \times \{0, \dots, N-1\}$  onto  $\{0, \dots, N^2-1\}$ . Let  $\mathbf{F}$  be an  $N^2 \times N^2$  matrix whose elements satisfy

$$\mathbf{F}_{(l,m),\langle u,v \rangle} = e^{-\frac{2\pi j}{N}(ul+vm)}. \quad (6)$$

Let  $\boldsymbol{\xi} = \text{vec}(\mathbf{V})$  and let  $\mathbf{t} = \text{vec}(\mathbf{I})$ . We have

$$\boldsymbol{\xi} = \mathbf{F}\mathbf{t}. \quad (7)$$

Note that  $\mathbf{t}$  is a real vector since the visibility measurements satisfy  $V(u, v) = V(-u, -v)$ . To make the problem real we define  $\mathbf{F}_R = \text{Re}(\mathbf{F})$ ,  $\mathbf{F}_I = \text{Im}(\mathbf{F})$  and variables  $\boldsymbol{\xi}_R = \text{Re}(\boldsymbol{\xi})$ ,  $\boldsymbol{\xi}_I = \text{Im}(\boldsymbol{\xi})$ . (7) now becomes

$$\begin{aligned} \boldsymbol{\xi}_R & = \mathbf{F}_R \mathbf{t} \\ \boldsymbol{\xi}_I & = \mathbf{F}_I \mathbf{t} \end{aligned} \quad (8)$$

For the measured locations  $(u_i, v_i)$  we have:

$$\begin{aligned}\xi_R(\langle u_i, v_i \rangle) &= \text{Re}(V_{\text{Measured}}(u_i, v_i)) & i = 1, \dots, M \\ \xi_I(\langle u_i, v_i \rangle) &= \text{Im}(V_{\text{Measured}}(u_i, v_i)) & i = 1, \dots, M\end{aligned}\quad (9)$$

where  $M$  is the number of given measurements in the  $(u, v)$  domain. The linear programming problem is described in Table 1.

$\min_{\mathbf{t}} \sum_{i=1}^{N^2} t_i$ <p>Subject to</p> $\xi_R(\langle u_i, v_i \rangle) = \text{Re}(V_{\text{Measured}}(u_i, v_i))$ $\xi_I(\langle u_i, v_i \rangle) = \text{Im}(V_{\text{Measured}}(u_i, v_i))$ $\mathbf{0} \leq \mathbf{t}$
---

**Table 1.**  $\ell_1$  optimization using linear programming

#### 4. SIMULATION RESULTS

In this section we demonstrate the performance of  $\ell_1$  reconstruction on a sparse image. The simulation was done in two steps. The first step is the radio telescope simulation. In this simulation the visibility was generated according to the original image, earth rotation and the radio telescope structure. From the visibility measurements the dirty image was produced. In the second step, reconstruction of the dirty image was done using  $\ell_1$  minimization (Table 1).

The simulated radio telescope is an east-west array containing 14 antennas logarithmically spaced from 1 to  $200\lambda$ . The visibility was calculated according to the simulated image  $I(l, m)$ . Noise was added to the visibility measurements, the SNR was  $-20\text{dB}$  per visibility measurement and 12 hours observation has been used. A gridding was performed using the pillbox convolution function. The dirty image was then calculated from measured visibility (after gridding). Image reconstruction was done using linear programming. We have used the CVX minimization package by Grant et al. [20]. Example of the image reconstruction performance is given in figures 2 and 3. Sub-figure (2(a)) depicts the original (simulated) image containing three sources: a point source, a Y shape source with intensity varying tail and a point source surrounded by a bright ring. Sub-figure (2(b)) shows the dirty image, the Y shape source is smeared and the tail loses the intensity structure, the ring is weakly seen. The reconstructed image is shown in sub-figure (2(c)), all three sources reconstructed. The Y shape is clearly seen (including the intensity structure in the tail), the ring is clearly seen and the point source intensity is reconstructed. Cross-sections location marked at sub-figure (3(a)). A cross section of the images throughout the ring is displayed at sub-figure (3(b)). At the original image the ring intensity is half the size of the central source. In the dirty image the ring is significantly weaker and

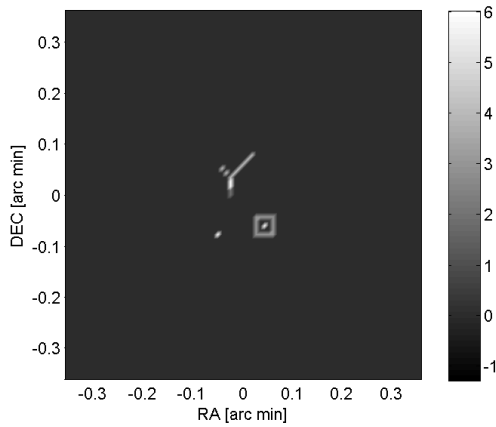
has negative parts. The ring intensity is reconstructed (almost half the size of the central source in the reconstructed image) and the negative parts vanishes. A cross-section of the Y shape source tail is displayed at sub-figure (3(c)). At the original image the tail has two levels of intensity, this intensity structure is smeared in the dirty image, and reconstructed by the  $\ell_1$  optimization

#### 5. CONCLUSIONS

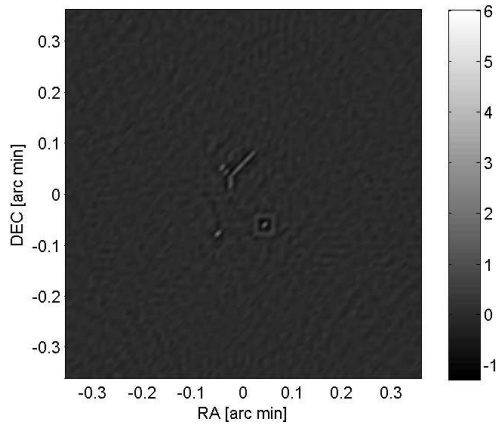
In this paper we proposed the use of  $\ell_1$  minimization for radio astronomical images. We showed that the  $\ell_1$  deconvolution can be solved by linear programming, and demonstrated the method on simulated sky model. The great potential of the methods proposed in this paper is a first step, towards the development of more advanced imaging techniques, capable of providing higher dynamic range and interference immunity as required by the radio telescopes of the future.

#### 6. REFERENCES

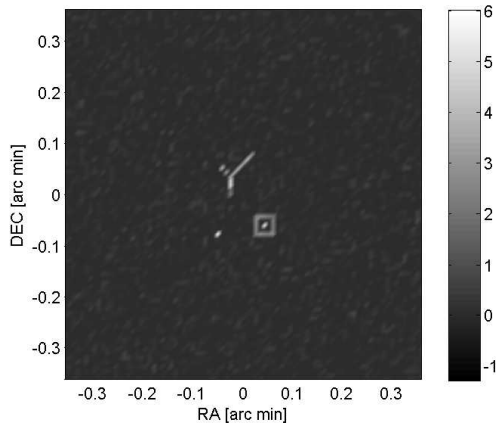
- [1] P.J. Hall, ed., *The Square Kilometer Array: An Engineering Perspective*. Springer, 2005. Reprinted from *Experimental Astronomy* Vol.17, 1-3, 2004.
- [2] J.D. Bregman, "LOFAR approaching the critical design review," in *Proceedings of the XXVIIIth General Assembly of the URSI*, 2005.
- [3] A.R. Thompson, J.M. Moran, and G.W. Swenson, eds., *Interferometry and Synthesis in Radio astronomy*. John Wiley and Sons, 1986.
- [4] J.A. Hogbom, "Aperture synthesis with non-regular distribution of interferometer baselines," *Astronomy and Astrophysics Supp.*, vol. 15, pp. 417–426, 1974.
- [5] E.T. Jaynes *Physics Review*, vol. 106, p. 620, 1957.
- [6] G. B. Taylor, C. L. Carilli, and R. A. Perley, *Synthesis Imaging in Radio-Astronomy*. Astronomical Society of the Pacific, 1999.
- [7] B.R. Frieden, "Restoring with maximum likelihood and maximum entropy," *Journal of the Optical Society of America*, vol. 62, pp. 511–518, 1972.
- [8] S.F. Gull and G.J. Skilling, "Image reconstruction from incomplete and noisy data," *Nature*, vol. 272, pp. 686–690, 1978.
- [9] D. S. Briggs, *High fidelity deconvolution of moderately resolved sources*. PhD thesis, The new Mexico Institute of Mining and Technology, Socorro, New Mexico, 1995.



(a) Original image

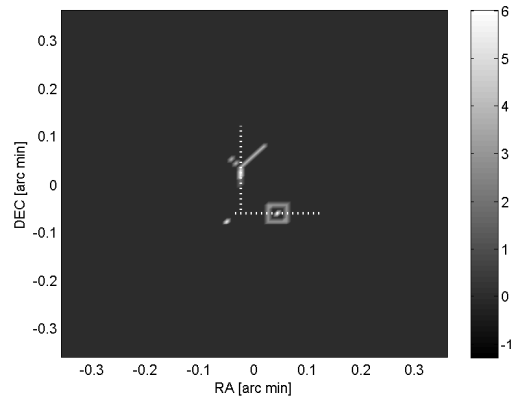


(b) Dirty image

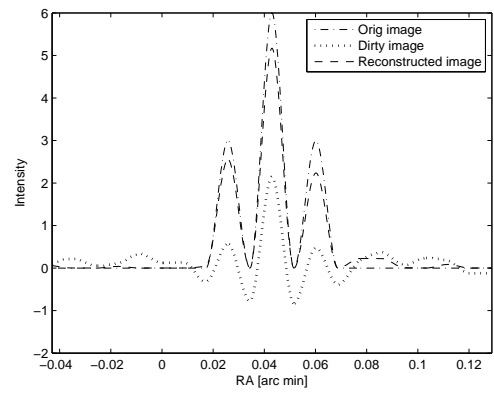


(c) Reconstructed image

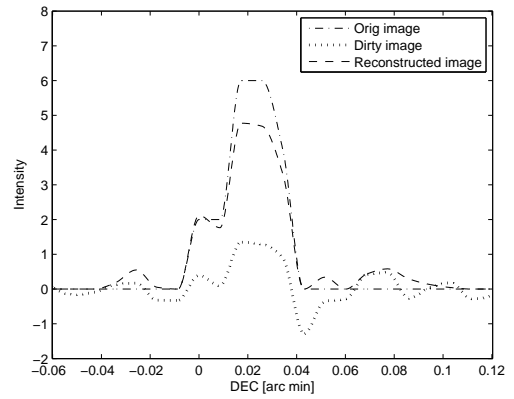
**Fig. 2.** Example of reconstruction results. (a) The true image (simulated). (b) The dirty image. (c) The reconstructed image.



(a) Cross-section location



(b) Cross-section throughout the ring



(c) Cross-section of the Y shape source tail

**Fig. 3.** Two cross-sections of the original image, dirty image and the reconstructed image. (a) cross-sections location (b) cross-section throughout the ring. (c) cross-section of the Y shape source tail

- [10] A. Leshem and A.J. van der Veen, "Radio-astronomical imaging in the presence of strong radio interference," *IEEE Trans. on Information Theory, Special issue on information theoretic imaging*, pp. 1730–1747, 2000.
- [11] A.J. van der Veen, A. Leshem, and A.J. Boonstra, "Array signal processing in radio-astronomy," *Experimental Astronomy*, 2004.
- [12] C. Ben-David and A. Leshem, "Radio astronomical imaging - parametric and non-parametric high resolution techniques," *IEEE Journal on Selected Topics in Signal Processing*, Oct 2008.
- [13] K. A. Marsh and J. M. Richardson, "The objective function implicit in the CLEAN algorithm," *Astronomy and Astrophysics (ISSN 0004-6361)*, vol. 182, pp. 174–178, Aug 1987.
- [14] D. C. Dobson and F. Santosa, "Recovery of blocky images from noisy and blurred data," *SIAM Journal on Applied Mathematics*, vol. 56, no. 4, pp. 1181–1198, 1996.
- [15] S. S. Chen, D. L. Donoho, and M. A. Saunders, "Atomic decomposition by basis pursuit," *Siam J. Sci Comput.*, vol. 20, no. 1, pp. 33–61, 1998.
- [16] A. Feuer and A. Nemirovski, "On sparse representation in pairs of bases," *IEEE transactions on information theory*, vol. 49, pp. 1579–1581, June 2003.
- [17] M. Elad and A. M. Bruckstein, "A generalized uncertainty principle and sparse representation in pairs of bases," *IEEE transactions on information theory*.
- [18] M. Rudelson and R. Vershynin, "Sparse reconstruction by convex relaxation: Fourier and gaussian measurements," Mar 2006.
- [19] E. Candes, J. Romberg, and T. Tao, "Robust uncertainty principles: Exact signal reconstruction from highly incomplete frequency information," *IEEE transactions on information theory*, vol. 52, pp. 489–509, February 2006.
- [20] M. Grant, S. P. Boyd, and Y. Ye, "CVX - Matlab software for disciplined convex programming. <http://www.stanford.edu/boyd/>".